Bode Analysis of Uncertain Multivariable Systems

Oomen, T.A.E.; Tacx, Paul

DOI
10.23919/ACC53348.2022.9867220

Publication date
2022

Document Version
Final published version

Published in
Proceedings of the American Control Conference (ACC 2022)

2022 American Control Conference (ACC)
Atlanta, USA, June 8-10, 2022

Bode Analysis of Uncertain Multivariable Systems

Paul Tacx and Tom Oomen

Abstract— **Bode plots are crucial for frequency domain analysis of SISO systems. The aim of this paper is to develop a complete approach for Bode plots of multivariable uncertain systems for both the magnitude and phase. The magnitude is based on the singular values. The phase is based on the phase spread of the numerical range. An IQC-based approach is pursued to provide both the magnitude and phase. A simulation example shows that the presented approach allows the generation of multivariable Bode plots of multivariable uncertain systems.**

I. INTRODUCTION

Models are inherently subject to uncertainty and robustness to these uncertainties is of vital importance in control design. This typically comes from parameter uncertainty or unmodeled dynamics. Robust control explicitly addresses model uncertainty by considering a model set. The availability of reliable and systematic robust control algorithms has spurred the development of identification approaches of multivariable model sets for robust control, see [1], [2], [3], [4]. However, the multivariable aspect and the trend towards more advanced uncertainty structures complicates uncertainty structure comparison, understanding, controller design, and performance analysis of uncertain systems. For this reason, visualizing multivariable uncertain systems is essential.

The Bode plot is a critical tool for understanding, controller design, and performance analysis of control systems [5], [6]. The Bode plot of SISO systems is based on the polar description of the complex number. Consequently, the Bode plot contains the magnitude and phase. The combination of magnitude and phase provides essential information regarding performance and stability including gain and phase margin. The close relationship between magnitude and phase is underlined by the Bode gain-phase relation [7]. Frequency response function-based approaches are also used in for example, for non-linear systems [8] and LPTV systems [9].

Bode plots for SISO nominal systems are well developed, but extensions to the multivariable case are not straightforward. An element-wise Bode plot is often considered for MIMO systems based on the matrix elements [1]. However, the element-wise Bode plot becomes unclear if the number of inputs and outputs increases. Consequently, a multivariable Bode plot is essential.

In sharp contrast to the multivariable magnitude, a multivariable phase definition has received substantially less attention. The multivariable magnitude is often based on the singular value, which are also referred to as principal magnitude [7], [5]. In [10], the scalar polar description is extended to a multivariable polar description. The multivariable polar description is used to define the principal magnitude and principal phase in [5]. The principal magnitude and phase define a principal region which are known to contain the characteristic loci. Consequently, analogous to the scalar polar decomposition, the multivariable polar description intuitively connects the multivariable magnitude and phase to stability. This property might be used for developing a multivariable phase margin.

Alternatively, Bode magnitude plots using singular value decompositions have been further developed towards uncertain systems [11], [12]. In [13], such generalizations are made based on the generalized and skewed structured singular values. However, a Bode phase equivalent is lacking.

The principal phase is a suitable measure of multivariable phase, yet extending the principal phase to uncertain systems is not straightforward. The key obstruction of the principal phase for uncertain systems is that the underlying eigenvalue problem is not necessarily convex. Eigenvalues are often approximated by the numerical range, which is convex [10]. In [14], the numerical range is used to define the minimum and maximum phase, i.e., phase spread. In [15], [14], [16] the phase spread is used for performance and stability analysis of uncertain systems. The phase spread introduces some conservatism with respect to the principal phase. However, for normal matrices, including SISO and diagonal systems, the phase spread is exact [14]. For many MIMO applications, systems are close to diagonal in the relevant frequency ranges [17, Sec. 2.1]. In addition, for the element-wise Bode plot, SISO results hold.

Although several results are available to analyze the magnitude and phase for multivariable uncertain systems, at present a unified approach for constructing Bode plots of uncertain multivariable systems is lacking. The main contributions of the paper are the following.

C1 A unified approach for MIMO uncertain Bode plots.
  C1.1 Element-wise Bode magnitude and phase.
  C1.2 Multivariable Bode magnitude and phase.

C2 A relevant simulation example.

Compared to [13], this paper considers an Integral Quadratic Constraints (IQC)-based approach to calculate the

*This work is part of the research programme VIDI with project number 15698, which is (partly) financed by the Netherlands Organisation for Scientific Research (NWO).

Paul Tacx is with the Control Systems Technology Group, Departement of Mechanical Engineering, Eindhoven University of Technology, Eindhoven, The Netherlands, e-mail: p.j.m.m.tacx@tue.nl.

Tom Oomen is with the Control Systems Technology Section, Department of Mechanical Engineering, Eindhoven University of Technology, Eindhoven, The Netherlands. He is also with the Delft Center for Systems and Control, Delft University of Technology, Delft, The Netherlands.

multivariable magnitude. This paper extends to the results in [15], [14], [16] as the multivariable phase definition is extended to construct Bode phase plots. To compute the multivariable phase, an IQC-based approach is pursued. The combination of the multivariable magnitude and phase leads to a unified approach for constructing multivariable Bode plots of uncertain systems. As a special case, the results in [5], [13], [14], [16], [15] are recovered.

This paper is organized as follows. In Section III, the problem considered in this paper is introduced. A multivariable magnitude and phase definition for multivariable Bode plots are introduced in Section IV. In Section V, the approach to generate the multivariable Bode plots is proposed. The new approach is applied in a simulation example in Section VI. Lastly, the conclusion is provided in Section VII.

II. Notation

The following notation is used throughout. For a matrix M, the transpose and complex conjugate transpose are denoted by $M^\top$ and M^* respectively. A matrix X is normal if $XX^* = X^*X$. For a matrix M, $M > (\geq)0$ and $M < (\leq)0$ denote positive (semi)definiteness and negative (semi)definiteness. For a matrix X, $\sigma(X)$, $\lambda(X)$, $\overline{\sigma}(X)$ and $\underline{\sigma}(X)$ denotes the singular values, eigenvalues, largest and smallest singular value respectively. The upper linear fractional transformation (LFT) is given by $\mathcal{F}_u(\hat{H}, \Delta_u) = \hat{H}_{22} + \hat{H}_{21}\Delta_u \left(I - \hat{H}_{11}\Delta_u\right)^{-1} \hat{H}_{12}$.

III. Problem Formulation

A. Preliminary: Bode Plots of Multivariable Systems

The Bode plot of a scalar LTI system with the transfer function $P(s) \in \mathcal{R}$ is a graphical representation of the complex frequency response of the system. The Bode plot is a combination of the Bode magnitude and phase plot which are constructed by plotting the magnitude $\left|P(s)\right|$ and phase $\arg\left(P(s)\right)$ on $s = j\omega$ for a grid of frequencies $\omega \in \Omega_d$. The frequency grid Ω_d is defined by the control engineer based on the frequency range of interest and should be sufficiently dense to capture potential resonances. Essentially, the magnitude and phase are based on the polar description of a complex number

$$z = r\exp(j\theta) \tag{1}$$

where $r > 0$ denotes the magnitude and $\theta \in [0, 2\pi)$ denotes the phase.

A multivariable magnitude and phase definition is essential for the development of a multivariable Bode plot. Analogous to the polar form of a scalar, the polar decomposition of a square matrix $P \in \mathbb{C}^{n\times n}$ is defined as [10]

$$P = UH_R, \tag{2}$$

$$P = H_L U, \tag{3}$$

where U is unitary and the matrices H_R and H_L are Hermitian. The matrices U, H_R, and H_L can be determined from the singular value decomposition

$$P = \Phi\Sigma\Psi^* \tag{4}$$

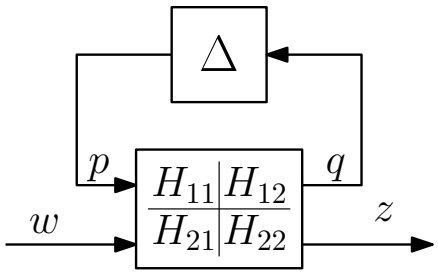

Fig. 1. Upper LFT plant setup.

where $U = \Phi\Psi^*$, $H_R = \Psi\Sigma\Psi^*$, and $H_L = \Phi\Sigma\Phi^*$. The multivariable magnitude of P are the eigenvalues of the Hermitian part H_L or H_R of the polar decomposition [10]

$$\sigma(P) = \lambda(H_R) = \lambda(H_L). \tag{5}$$

The multivariable magnitude coincides with the widely accepted definition of multivariable magnitude, the singular values of P. Although a widely accepted multivariable phase definition does not exist, a multivariable phase definition based on the multivariable polar description exists. The principal phases of the matrix P are defined as the arguments of the eigenvalues of the unitary part U [10], given by

$$\psi(P) = \arg\left\{\lambda(U)\right\}. \tag{6}$$

A multivariable Bode plot can be constructed by computing the principal magnitude and phase for each frequency in the frequency grid Ω_d.

Remark 1: In this paper, square systems are considered. However, the principal magnitude can be extended to nonsquare systems by adding auxiliary zero rows or columns such that a square system is obtained. This procedure essentially boils down to the singular values of nonsquare matrices. In sharp contrast, extending the principal phase to nonsquare systems is not straightforward. A multivariable phase can potentially be defined based on a numerical range for nonsquare systems, see [18].

B. Uncertain Systems

Consider the uncertain multivariable model set $\mathcal{P}$. The model set is based on the LFT in Fig. 1, i.e.,

$$\begin{pmatrix} q \\ z \end{pmatrix} = \begin{pmatrix} \hat{H}_{11} & \hat{H}_{12} \\ \hat{H}_{21} & \hat{H}_{22} \end{pmatrix} \begin{pmatrix} p \\ w \end{pmatrix}. \tag{7}$$

The channel $w \mapsto z$ is referred to as the performance channel and $p \mapsto q$ is the uncertainty channel with $p = \Delta q$. The structure of the model set is defined by the transfer matrices $\hat{H}_{11}$, $\hat{H}_{12}$, $\hat{H}_{21}$, and $\hat{H}_{22}$. The model set is defined as

$$\mathcal{P} = \left\{P \middle| P = \mathcal{F}_u\left(H, \Delta\right)\right\}, \tag{8}$$

where the uncertainty $\Delta \in \mathbf{\Delta}$ is an $\mathcal{H}_\infty$-norm bounded subset [19]

$$\begin{aligned}\mathbf{\Delta} = \big\{\Delta \in \mathcal{RH}_\infty \big| \, \|\Delta\|_\infty \leq \gamma, \\ \text{blockdiag}(\delta_1, ..., \delta_{n_d}, \Delta_1, ..., \Delta_{n_u})\big\}.\end{aligned} \tag{9}$$

The parameter γ defines the $\mathcal{H}_\infty$-norm bound, $\delta_i \in \mathbb{C}$ and $\Delta_i \in \mathbb{C}^{p_i \times p_i}$. The uncertainty set can be subject to additional constraints, such as parameter uncertainty from a polytope [20], [21].

C. Problem Formulation

The aim of this paper is to develop a unified approach to construct multivariable Bode plots of uncertain systems. The key idea is to extend the multivariable magnitude and phase definition based on the multivariable polar decomposition to the uncertain case.

IV. Multivariable Magnitude and Phase Analysis

1) Multivariable Magnitude: The key idea for the computation of the multivariable magnitude of uncertain systems is to compute the minimum and maximum singular value of the uncertain system for each frequency in the frequency grid.

Definition 1: Let $\mathcal{P}$ be an uncertain system according to (8). For a fixed frequency ω the minimum and maximum magnitude are defined as

$$\underline{\xi}(\mathcal{P}) = \inf_{P \in \mathcal{P}} \underline{\sigma}\left(P(j\omega)\right), \tag{10}$$

$$\overline{\xi}(\mathcal{P}) = \sup_{P \in \mathcal{P}} \overline{\sigma}\left(P(j\omega)\right). \tag{11}$$

By calculating $\underline{\xi}(\mathcal{P})$ and $\overline{\xi}(\mathcal{P})$ for each frequency in the frequency range of interest, a multivariable Bode magnitude plot is constructed.

2) Multivariable Phase: Although the principal phase is a suitable multivariable phase definition, extending to uncertain systems is not straightforward. The key reason is that the underlying eigenvalue problem in (6) is not necessarily convex. For this reason, the numerical range

$$\mathcal{W}(P) = \{x^* P x | x \in \mathbb{C}^n, \|x\| = 1\} \tag{12}$$

is considered [10], [14]. The key benefit of the numerical range is that the set $\mathcal{W}(P)$ is convex. Furthermore, the numerical range is known to contain the spectrum of a matrix [10].

The numerical range allows generating a multivariable phase definition which allows to approximating the principal phase for uncertain systems. To construct such a multivariable phase definition, the numerical range is extended to the uncertain case by considering the union of the numerical ranges $\mathcal{W}(P)$ for $P \in \mathcal{P}$. Next, consider a cone in the complex plane that contains numerical ranges of the uncertain system $\mathcal{P}$. The cone is centered in the origin and is described by two angles $\underline{\phi}(\mathcal{P})$ and $\overline{\phi}(\mathcal{P})$ as indicated in Fig. 2. The key challenge is to find the smallest cone that contains the union of numerical ranges. The angles $\underline{\phi}(\mathcal{P})$ and $\overline{\phi}(\mathcal{P})$ define the multivariable phase.

Definition 2: Let $\mathcal{P}$ be an uncertain system according to (8). Assume the union of numerical ranges of $\mathcal{P}$ to be in the right half-plane. For a fixed frequency ω the minimum and maximum multivariable phase are defined as

$$\underline{\phi}(\mathcal{P}) = \inf_{P \in \mathcal{P}} \left\{ \inf_{\kappa \in \mathcal{W}(P)} \arg\{\kappa\} \right\}, \tag{13}$$

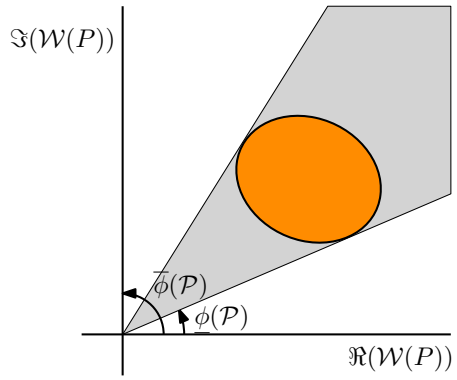

Fig. 2. Union of numerical ranges $\mathcal{W}(P), \forall P \in \mathcal{P}$ (orange) and cone defined by the multivariable phases $\underline{\phi}(\mathcal{P})$ and $\overline{\phi}(\mathcal{P})$ (grey).

$$\overline{\phi}(\mathcal{P}) = \sup_{P \in \mathcal{P}} \left\{ \sup_{\kappa \in \mathcal{W}(P)} \arg\{\kappa\} \right\}, \tag{14}$$

Throughout, without loss of generality, the numerical range is assumed to be contained in the right half-plane. If the numerical range is not in the right half-plane, the numerical range is rotated by an angle ν such that $\mathcal{W}(\exp(j\nu)P(j\omega_0))$ is in the right half-plane for all $P \in \mathcal{P}$.

Remark 2: If the phase spread, i.e., the difference between the minimum and maximum phase, is larger than π, the phase is contained in a range of 2π. This is the case if the numerical range contains the origin.

Remark 3: The multivariable phase based on the numerical range approximates the principal phase. Specifically, the numerical range-based phase bounds the principal phase from below and above

$$\overline{\phi}(P) \geq \psi(P), \qquad \underline{\phi}(P) \leq \psi(P). \tag{15}$$

If the matrix P is normal, then the inequalities become equalities, i.e., $\mathcal{W}(P)$ equals the convex hull of the spectrum of P [14]. Consequently, if a SISO, diagonal, or element-wise system is considered, the numerical range-based phase is exact.

3) Element-wise Magnitude and Phase: Consider the uncertain system $\mathcal{P}$ according to (8). The ij^{th} element of $\mathcal{P}$ is defined as

$$\mathcal{P}_{ij} = \{P_{ij} | P_{ij} \in u_i^* \mathcal{P} u_j\} \tag{16}$$

where u_l denotes a vector of appropriate length with the l-th element equal to one and all other elements zero. The multivariable magnitude of Def. 1 and phase of Def. 2 are easily extended to the element-wise case by considering the elements (16). As indicated in Remark 3, the numerical range-based phase is exact with respect to the principal phase in the element-wise case. The element-wise Bode magnitude and phase plot are also valid for nonsquare systems.

V. Main Result

This section aims to develop an approach to construct multivariable Bode plots of uncertain system which constitutes Contribution C1. To generate the Bode plots, an IQC-based approach is considered to determine the magnitude and phase are determined on a frequency-by-frequency basis.

A. Integral Quadratic Constraints (IQC)

The IQC framework is often used in Robust Control to analyze the uncertainty and performance channel in terms of relations between inputs and outputs. The first step in characterizing the performance is to capture the uncertainty channel $p \mapsto q$ in the IQC framework.

Definition 3: The signals $q(j\omega)$ and $p(j\omega)$ are said to satisfy the IQC defined by the multiplier $\{\Pi_{11}, \Pi_{12}, \Pi_{22}\}$ with $\Pi_{11} = \Pi_{11}^*$, $\Pi_{12} = \Pi_{12}^*$ and $\Pi_{22} = \Pi_{22}^*$ if

$$\int_{-\infty}^{\infty} \begin{pmatrix} q(j\omega) \\ p(j\omega) \end{pmatrix}^* \begin{pmatrix} \Pi_{11}(j\omega) & \Pi_{12}(j\omega) \\ \Pi_{12}^*(j\omega) & \Pi_{22}(j\omega) \end{pmatrix} \begin{pmatrix} q(j\omega) \\ p(j\omega) \end{pmatrix} d\omega \geq 0. \quad (17)$$

Note that in this paper LTI uncertain systems are considered. For this reason, the integral in (17) is dropped in the forthcoming. In addition, the magnitude and phase are determined on a frequency-by-frequency basis. For this reason, the results are developed based on a fixed frequency ω and the frequency dependence is dropped. Consequently, the IQC (17) can be reduced to

$$\begin{pmatrix} q \\ p \end{pmatrix}^* \begin{pmatrix} \Pi_{11} & \Pi_{12} \\ \Pi_{12}^* & \Pi_{22} \end{pmatrix} \begin{pmatrix} q \\ p \end{pmatrix} \geq 0. \quad (18)$$

For typical uncertainty structure, such as unstructured uncertainty or parameters from a polytope, matrices $\{\Pi_{11}, \Pi_{12}, \Pi_{22}\}$ are available, e.g., in [22], [21]. In case unstructured uncertainty is considered, see (9) without any structural constraints, then (17) holds for the matrix

$$\Pi_u = \text{blockdiag}\left(I, -\gamma^2 I\right). \quad (19)$$

The next step is to characterize the performance channel. For this purpose, consider the performance criterion

$$\begin{pmatrix} z \\ w \end{pmatrix}^* \begin{pmatrix} \Pi_{p,11} & \Pi_{p,12} \\ \Pi_{p,12}^* & \Pi_{p,22} \end{pmatrix} \begin{pmatrix} z \\ w \end{pmatrix} < 0. \quad (20)$$

The performance matrix Π_p satisfies $\Pi_{p,11} = \Pi_{p,11}^*$, $\Pi_{p,12} = \Pi_{p,12}^*$ and $\Pi_{p,22} = \Pi_{p,22}^*$. The following theorem presents a necessary and sufficient condition for the performance analysis of uncertain systems.

Theorem 1: Suppose that (18) is satisfied for a given Π for all $\Delta \in \mathbf{\Delta}$. The performance criterion (20) is satisfied for a Π_p if and only if

$$\begin{pmatrix} \hat{H}_{11} & \hat{H}_{12} \\ I & 0 \\ \hat{H}_{21} & \hat{H}_{22} \\ 0 & I \end{pmatrix}^* \begin{pmatrix} \Pi & 0 \\ 0 & \Pi_p \end{pmatrix} \begin{pmatrix} \hat{H}_{11} & \hat{H}_{12} \\ I & 0 \\ \hat{H}_{21} & \hat{H}_{22} \\ 0 & I \end{pmatrix} \prec 0. \quad (21)$$

A proof can be found in [23, Section 4].

B. IQC with Application to Magnitude and Phase

1) Magnitude: Finding the minimum and maximum singular value in Def. 1 can be formulated by computing the largest $\underline{\alpha}$ and smallest $\overline{\alpha}$ such that

$$\underline{\alpha}^2 w^* w - z^* z < 0, \quad (22)$$

$$-\overline{\alpha}^2 w^* w + z^* z < 0, \quad (23)$$

where w, z refer to the signals in (7). The parameters $\underline{\alpha}$ and $\overline{\alpha}$ define the interior and exterior respectively, of an annular region in the complex plane. The description of the input-output behavior can be formulated as IQC as shown in the following.

Theorem 2: Let H denote the multivariable system at frequency ω of the form (7) with its input w and output z. If the inequalities (22) and (23) hold, then (20) holds with the performance matrices

$$\Pi_{p,1} = \text{blockdiag}\left(-I, \underline{\alpha}^2 I\right), \quad (24)$$

$$\Pi_{p,2} = \text{blockdiag}\left(I, -\overline{\alpha}^2 I\right). \quad (25)$$

2) Phase: The computation of the minimum and maximum phase in Def. 2 can be reformulated by finding the largest $\underline{\beta}$ and smallest $\overline{\beta}$ such that

$$\Re\{w^* z\} > \frac{\Im\{w^* z\}}{\tan(\underline{\beta})}, \quad (26)$$

$$\Re\{w^* z\} < \frac{\Im\{w^* z\}}{\tan(\overline{\beta})}. \quad (27)$$

Essentially, the angles $\underline{\beta}$ and $\overline{\beta}$ in (26) and (27) define a cone in the complex plane. The largest $\underline{\beta}$ and smallest $\overline{\beta}$ correspond to the multivariable phases in (13) and (14). The inequalities in (27) and (27) can be reformulated to the IQC framework.

Theorem 3: Let H denote the multivariable system at frequency ω of the form (7) with its input w and output z. The inequalities in (26) and (27) hold if and only if the IQC (20) holds with the performance matrices

$$\Pi_{p,3} = \begin{pmatrix} 0 & -\sin(\underline{\beta}) + j\cos(\underline{\beta}) \\ -\sin(\underline{\beta}) - j\cos(\underline{\beta}) & 0 \end{pmatrix}, \quad (28)$$

$$\Pi_{p,4} = \begin{pmatrix} 0 & \sin(\overline{\beta}) - j\cos(\overline{\beta}) \\ \sin(\overline{\beta}) + j\cos(\overline{\beta}) & 0 \end{pmatrix}. \quad (29)$$

Essentially, Theorems 2 and 3 allow to rewrite the quadratic expressions (22), (23), (26), and (27) to matrix inequalities (21). In the next section, Theorems 2 and 3 are exploited to compute the multivariable magnitude and phase.

C. Magnitude and Phase Algorithm

In this section, the results of Sections V-A and V-B are exploited to develop an approach to generate Bode plots of uncertain multivariable systems.

Theorem 4: Let H be the system of the form (7), $\Delta \in \mathbf{\Delta}$ an uncertainty block of the form (9), and consider the fixed bounds $\underline{\alpha}$, $\overline{\alpha}$, and $\underline{\beta}$, $\overline{\beta}$. Suppose that (17) holds for the given matrices Π_{11}, Π_{12}, and Π_{22}. The performance matrices $\Pi_{p,i}$, $i \in \{1, .., 4\}$ are defined by (24), (25), (28) and (29). The matrix inequalities

$$F(\Pi_{p,i}) = \begin{pmatrix} \hat{H}_{11} & \hat{H}_{12} \\ I & 0 \\ \hat{H}_{21} & \hat{H}_{22} \\ 0 & I \end{pmatrix}^* \begin{pmatrix} \Pi & 0 \\ 0 & \Pi_{p,i} \end{pmatrix} \begin{pmatrix} \hat{H}_{11} & \hat{H}_{12} \\ I & 0 \\ \hat{H}_{21} & \hat{H}_{22} \\ 0 & I \end{pmatrix} \prec 0 \quad (30)$$

for $i \in \{1, ..., 4\}$ hold if and only if

$$\underline{\alpha} \leq \underline{\xi}(\mathcal{P}), \quad \overline{\xi}(\mathcal{P}) \leq \overline{\alpha}, \quad (31)$$

$$\underline{\beta} \leq \underline{\phi}(\mathcal{P}), \quad \overline{\phi}(\mathcal{P}) \leq \overline{\beta}. \quad (32)$$

Theorem 4 defines four feasibility problems for fixed bounds $\underline{\alpha}$, $\overline{\alpha}$, and $\underline{\beta}$, $\overline{\beta}$. Testing the feasibility problems is a linear matrix inequality that can be efficiently computed. Theorem 4 can be used to determine the magnitude and phase of uncertain systems. The minimum and maximum magnitude and phase (10), (11), (13), and (14) are determined by solving the following optimization problems

$$\underline{\xi}(\mathcal{P}) = \arg\max_{\underline{\alpha}} \left\{\underline{\alpha} | F(\Pi_{p,1}(\underline{\alpha})) \prec 0\right\}, \tag{33}$$

$$\overline{\xi}(\mathcal{P}) = \arg\min_{\overline{\alpha}} \left\{\overline{\alpha} | F(\Pi_{p,2}(\overline{\alpha})) \prec 0\right\}, \tag{34}$$

$$\underline{\phi}(\mathcal{P}) = \arg\max_{\underline{\beta}} \left\{\underline{\beta} \middle| F(\Pi_{p,3}(\underline{\beta})) \prec 0\right\}, \tag{35}$$

$$\overline{\phi}(\mathcal{P}) = \arg\min_{\overline{\beta}} \left\{\overline{\beta} \middle| F(\Pi_{p,4}(\overline{\beta})) \prec 0\right\}. \tag{36}$$

The optimization problems are solved by iterating over the parameters $\underline{\alpha}$, $\overline{\alpha}$ and $\underline{\beta}$, $\overline{\beta}$ through bisection. Since the bisection algorithm is used, the magnitudes and phases can be determined up to arbitrary precision. The multivariable Bode plot is constructed by computing the magnitude and phase for each frequency in the frequency grid. Consequently, the computations can be executed in parallel. The computational complexity is determined by the number of inputs and outputs, the number of iterations, and the size of the frequency grid.

VI. Example

This section shows that the proposed algorithm allows generating Bode plots of uncertain systems through a simulation example which constitutes contribution C2.

A. System

In the example, a MIMO mass-spring-damper system is considered with two inputs and two outputs with weak interaction. Fig. 3 depicts a Bode diagram of the true system P_o. The system P_o is stabilized by the experimental controller C_{exp} which delivers a reasonable bandwidth of 5 Hz. Furthermore, an eighth-order control-relevant nominal model $\hat{P}$ (Fig. 3) is estimated based on the algorithm in [1]. In the example, a specific model set is considered, the robust-control relevant model set [1]. The robust-control-relevant model set is defined as $\mathcal{P}^{RCR} = \mathcal{F}_u(\hat{H}^{RCR}, \Delta_u)$ with

$$\hat{H}^{RCR} = \begin{bmatrix} \hat{D}^{-1}N_C & \hat{D}^{-1} \\ D_C + \hat{P}N_C & \hat{P} \end{bmatrix} \tag{37}$$

where the pair $\{\hat{N}, \hat{D}\}$ is a right coprime factorization of the robust-control-relevant nominal model and the pair $\{N_c, D_c\}$ is a right coprime factorization of the experimental controller C_{exp}. Since the nominal model $\hat{P}$ does not capture the complete behavior of the true system P_o, a part of the dynamics is captured in the uncertainty. In this example, unstructured uncertainty is considered

$$\boldsymbol{\Delta_u} = \{\Delta_u \in \mathcal{RH}_\infty | \|\Delta_u\|_\infty \leq \gamma\}. \tag{38}$$

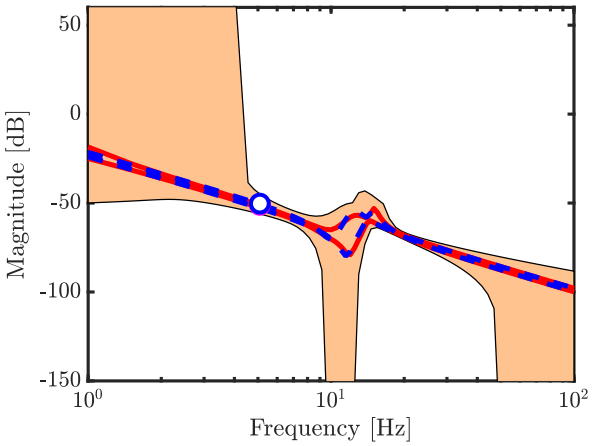

Fig. 3. Multivariable Bode magnitude plot of the true system P_o (——), the nominal model $\hat{P}$ (——) and the model set $\mathcal{P}$ (■). Bandwidth is indicated with the marker.

B. Result

The multivariable system is visualized using the techniques presented in this paper. The multivariable Bode magntiude and phase plot are depicted in Fig. 3 and 4. Here, the singular values of the true system P_o and nominal model $\hat{P}$ are shown. Furthermore, the minimum and maximum singular values of the model set $\mathcal{P}^{RCR}$ are depicted using the IQC-based algorithm of Section V-C. Iterations are stopped if an absolute convergence, i.e., the difference between the current and previous iteration, of -100dB is reached.

In the Bode phase plot, the principal phase of the true system and the nominal model are shown. In addition, the minimum and maximum phase of the model set is shown based on the algorithm presented in Section V-C. Iterations are stopped if an absolute convergence of 0.05° is achieved. The Bode plots reveal that the model set is tight around the desired cross-over frequency. However, at low frequencies, the model set is large and hence uncertain. A similar observation holds at higher frequencies. It is emphasized that this behavior is not caused by conservatism in the underlying algorithm. This specific behavior is attributed to the control-relevant coprime factors which emphasize the frequency content important for achieving the desired performance.

The element-wise Bode magnitude and phase are depicted in Fig. 5 and 6. Here, the elements of the multivariable system are considered according to (16). The Bode magnitude and phase of the elements of the model set are computed by the algorithm presented in Section V-C. As pointed out in Section III-C, as the elements are considered, the numerical range-based phase is equal to the principal phase. Overall, the

VII. Conclusion

In this paper, a new approach is developed for constructing Bode plots of uncertain multivariable systems. This is achieved by exploiting the multivariable extension of the polar description. This results in a multivariable magnitude

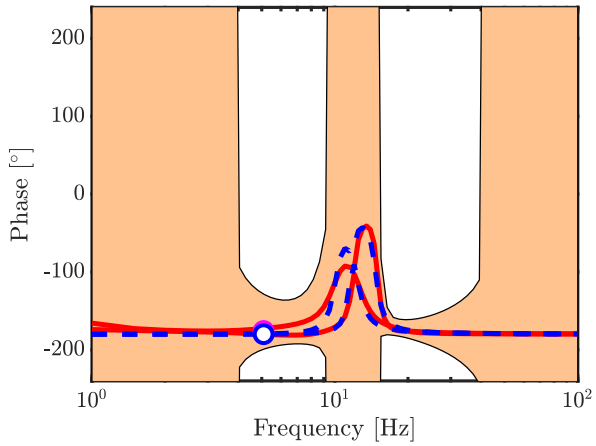

Fig. 4. Multivariable Bode phase plot: principal phase of the true system P_o (——) and the nominal model $\hat{P}$ (——), and numerical range-based phase of the model set $\mathcal{P}$ (■). Bandwidth is indicated with the marker.

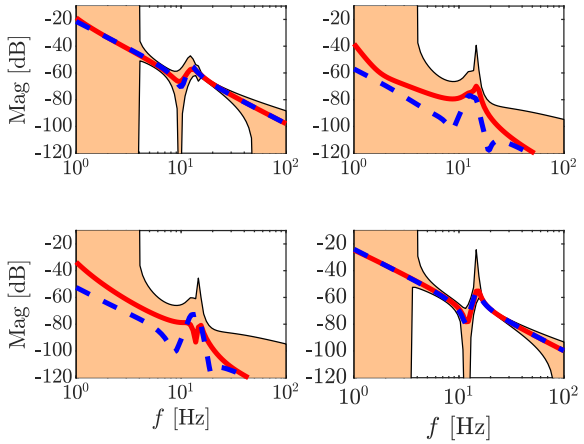

Fig. 5. Element-wise Bode magnitude plot of the true system P_o (——), the nominal model $\hat{P}$ (——) and the model set $\mathcal{P}$ (■).

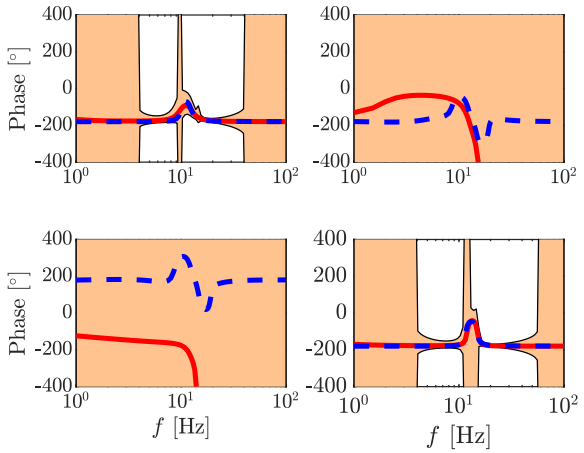

Fig. 6. Element-wise Bode phase plot based of the true system P_o (——), the nominal model $\hat{P}$ (——) and the model set $\mathcal{P}$ (■).

based on the singular values. The multivariable phase is based on the numerical range. To construct the Bode magnitude and phase plot, an IQC-based algorithm is proposed. A simulation example shows that the presented approach allows the generation of multivariable Bode plots of multivariable uncertain systems.

REFERENCES

[1] T. Oomen, R. van Herpen, S. Quist, M. van de Wal, O. Bosgra, and M. Steinbuch, "Connecting system identification and robust control for next-generation motion control of a wafer stage," *IEEE Trans. on Contr. Sys. Tech.*, vol. 22, no. 1, pp. 102–118, 2013.

[2] R. A. De Callafon and P. M. Van den Hof, "Suboptimal feedback control by a scheme of iterative identification and control design," *Mathematical modelling of systems*, vol. 3, no. 1, pp. 77–101, 1997.

[3] H. Hjalmarsson, "From experiment design to closed-loop control," *Automatica*, vol. 41, no. 3, pp. 393–438, 2005.

[4] M. Gevers, "Identification for control: From the early achievements to the revival of experiment design," *European journal of control*, vol. 11, no. 4-5, pp. 335–352, 2005.

[5] I. Postlethwaite, J. Edmunds, and A. MacFarlane, "Principal gains and principal phases in the analysis of linear multivariable feedback systems," *IEEE Trans. on Autom. Contr.*, vol. 26, no. 1, pp. 32–46, 1981.

[6] H. M. James, N. B. Nichols, and R. S. Phillips, *Theory of servomechanisms*. McGraw-Hill New York, 1947, vol. 25.

[7] S. Skogestad and I. Postlethwaite, *Multivariable feedback control: analysis and design*. Citeseer, 2007, vol. 2.

[8] A. Pavlov, N. van de Wouw, and H. Nijmeijer, "Frequency response functions for nonlinear convergent systems," *IEEE Trans. Autom. Control*, vol. 52, no. 6, pp. 1159–1165, 2007.

[9] T. Oomen, M. van de Wal, and O. Bosgra, "Design framework for high-performance optimal sampled-data control with application to a wafer stage," *Int. J. Control*, vol. 80, no. 6, pp. 919–934, 2007.

[10] F. Gantmacher, *The theory of matrices*. Chelsea, 1959, vol. 1.

[11] J. Doyle and G. Stein, "Multivariable feedback design: Concepts for a classical/modern synthesis," *IEEE Trans. on Autom. Control*, vol. 26, no. 1, pp. 4–16, 1981.

[12] M. Newlin and R. Smith, "A generalization of the structured singular value and its application to model validation," *IEEE Trans. Autom. Control*, vol. 43, no. 7, pp. 901–907, 1998.

[13] T. Oomen, S. Quist, R. van Herpen, and O. Bosgra, "Identification and visualization of robust-control-relevant model sets with application to an industrial wafer stage," in *49th IEEE CDC*. IEEE, 2010, pp. 5530–5535.

[14] D. Owens, "The numerical range: A tool for robust stability studies," 1984.

[15] K. Laib, A. Korniienko, M. Dinh, G. Scorletti, and F. Morel, "Hierarchical robust performance analysis of uncertain large scale systems," *IEEE Trans. Autom. Contr.*, vol. 63, no. 7, pp. 2075–2090, 2017.

[16] A. L. Tits, V. Balakrishnan, and L. Lee, "Robustness under bounded uncertainty with phase information," *IEEE Trans. Autom. Contr.*, vol. 44, no. 1, pp. 50–65, 1999.

[17] M. Van de Wal, G. van Baars, F. Sperling, and O. Bosgra, "Multivariable $\mathcal{H}_\infty/\mu$ feedback control design for high-precision wafer stage motion," *Control engineering practice*, vol. 10, no. 7, pp. 739–755, 2002.

[18] A. Aretaki and J. Maroulas, "Investigating the numerical range of non square matrices," 2009.

[19] A. Packard and J. Doyle, "The complex structured singular value," *Automatica*, vol. 29, no. 1, pp. 71–109, 1993.

[20] G. E. Dullerud and F. Paganini, *A course in robust control theory: a convex approach*. Springer Science & Business Media, 2013, vol. 36.

[21] A. Megretski and A. Rantzer, "System analysis via integral quadratic constraints," *IEEE Trans. Autom. Control*, vol. 42, no. 6, pp. 819–830, 1997.

[22] J. Veenman, C. W. Scherer, and H. Köroğlu, "Robust stability and performance analysis based on integral quadratic constraints," *European Journal of Control*, vol. 31, pp. 1–32, 2016.

[23] G. Scorletti, "Robustness analysis with time-delays," in *36th IEEE CDC*, vol. 4, 1997, pp. 3824–3829 vol.4.